



# DESIGN AND TESTING OF A COMPACT INEXPENSIVE PROTOTYPE REMOTELY OPERATED UNDERWATER VEHICLE FOR SHALLOW WATER OPERATION

A. Tanveer<sup>1,2</sup> and S. M. Ahmad<sup>3,4</sup>

<sup>1</sup>Department of Mechanical & Aerospace Engineering, Institute of Avionics & Aeronautics, Air University, Islamabad 44000, Pakistan, [ahsan.tanveer@mail.au.edu.pk](mailto:ahsan.tanveer@mail.au.edu.pk)

<sup>2</sup>Faculty of Mechanical Engineering, Ghulam Ishaq Khan Institute of Engineering Sciences and Technology, Topi 23640, Pakistan, [ahsantanveer3883@gmail.com](mailto:ahsantanveer3883@gmail.com)

<sup>3</sup>Control & Instrumentation Engineering Department, King Fahd University of Petroleum and Minerals, Dhahran 31261, Saudi Arabia, [sarvat.ahmad@kfupm.edu.sa](mailto:sarvat.ahmad@kfupm.edu.sa)

<sup>4</sup>Interdisciplinary Research Center for Intelligent Manufacturing and Robotics, King Fahd University of Petroleum and Minerals, Dhahran 31261, Saudi Arabia

## Abstract:

*This article focuses on a small and cost-effective remotely operated unmanned underwater vehicle (ROV) that has the ability to move through shallow waters. The proposed ROV measures 35 cm × 26 cm × 23 cm and weighs 1.59 kg. The primary objective is to remotely communicate in real time using serial protocol to record the vehicle's orientation data. The three DC motors powering the ROV are controlled by a multi-parameter root-locus proportional-integral (MRPL-PI) controller. Utilizing the processing capabilities of the Atmega328 microcontroller, heading, depth control, and water condition monitoring are all accomplished simultaneously. The Arduino development environment is used to establish the ROV's remote control. The problem with human divers who can only descend to a depth of 30 meters is resolved by the proposed ROV's ability to dive up to 100 meters underwater. Also, the suggested vehicle can be beneficial in marine applications such as measurement, maintenance, operations, and surveillance. Furthermore, the preliminary testing carried out in the pool indicates that the vehicle is fully operational and responds to the pilot's commands efficiently.*

**Keywords:** remotely operated underwater vehicle, marine robotics, proportional—integral controller, affordable ROVs, underwater exploration

## NOMENCLATURE

$K_p$	proportional gain	$P$	pressure/depth
$\alpha$	weighing factor for complementary filter	$\rho$	density of water

## 1. Introduction

Human Divers and manned underwater vehicle have increasingly been supplanted by ROVs due to the hazards to human life that come with underwater work. The fundamental reason for the increasing popularity of ROVs over the past several years is that, in addition to safety, they have provided a more efficient and affordable way for undersea research. Numerous ROV studies have recently been published with applications in ocean research (Tanveer & Ahmad, 2022), (Li et al., 2023), (Dong & Duan, 2023). ROVs have been employed for underwater maintenance operations, naval defense, and marine research (Capocci et al., 2017), (Khojasteh & Kamali, 2017). The majority of research efforts, however, have been directed at underwater surveillance (Ferri et al., 2018), (Shahani et al., 2018). Other research studies have centered on gathering tidal data (Brito & Griffiths, 2018). Additionally, ROVs have been used to take images underwater (Sánchez-Ferreira et al., 2019). Considering the vast variety of specializations that are involved in obtaining optimal performance, research continues to be actively pursued despite substantial advancements that have been made in the development of ROVs. A prevalent topic in the marine robotic community right now is the development of affordable vehicles without compromising functionality (Teague et al., 2018). Some of the domains where current research is impacting include the autonomy of the ROV, energy efficiency, and communication reliability (Cely et al., 2019),

(Martorell-Torres et al., 2018), (Xu et al., 2018). However, in the last few years, there has been an increasing trend towards creating affordable and easily accessible marine robotic platforms. In recent times, there have been various attempts to create affordable underwater robotic platforms, such as the one in (Laidani et al., 2022), and (Zhang et al., 2022). Various Pakistani researchers have also made efforts to develop a low-cost ROV, with success achieved by (Rafi et al., 2018), and (Shah et al., 2021). While these systems offer cost-effective solutions, it remains difficult to design a system that is suitable for academic purposes and uses widely accessible components.

In this article, we propose a low-cost and easy-to-replicate ROV that is capable of functioning as a fully operational underwater vehicle in calm waters. We suggest utilizing an Arduino Nano as an onboard computer since it is affordable, open-source, and supports C++. It is also recommended to add a complementary filter to the MPRL-PI controller. This contributes to the improved performance of the controller utilized for trajectory tracking. The remainder of this article is structured as follows: Section 2 details hardware organization, MPRL-PI controller development, and ROV mechanical design. The experimental findings are presented in Section 3, along with a comparison to commercial ROVs and details on ROV's performance in actual underwater environment. The conclusions of the article are finally summarized in Section 4.

## 2. ROV Design and Construction

### 2.1 Electronic Architecture Design

The hardware block diagram, which comprises of two components—the ROV and the ground station—is shown in Fig. 1. An Ethernet cable is used to transmit data between these two components. An Arduino Nano microcontroller, which forms the central part of the ROV hardware, is in charge of performing operations like measuring and recording various variables associated with the sensors and controlling motors. Additionally, the system includes two power sources: one is an Ethernet wire that provides 5 V to the Arduino Nano microcontroller and digital sensors, and the other is a dedicated line that provides 12 V to power two DC motors. The ROV has virtually limitless endurance with these power sources.

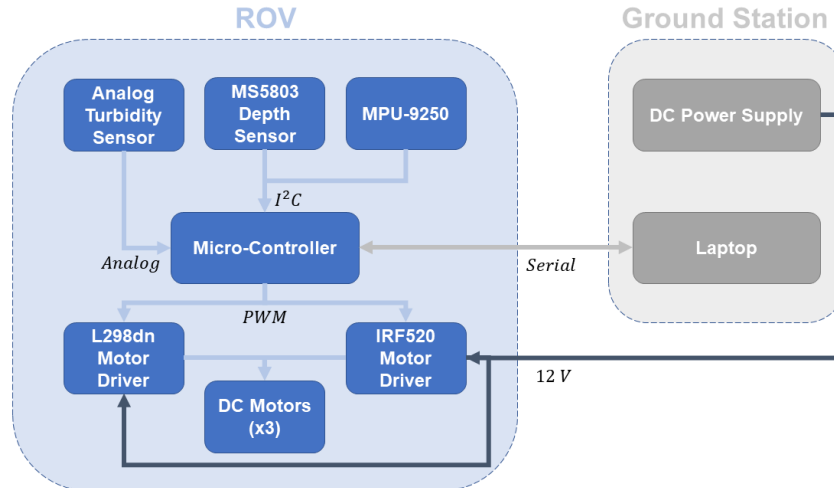


Fig. 1: ROV Electronic Architecture.

Motor drivers, which input pulse width modulation (PWM) signals produced by Arduino Nano microcontrollers, control DC motors. Typically, a bi-directional motor driver is needed for surge and yaw motion. However, it is often large in size. Unidirectional motor drivers, on the other hand, are fairly small in size but can only run motors in one direction. Onboard the ROV employed in this study are two distinct types of motor drivers. First a bi-directional L298dn which can power two motors simultaneously. Second a uni-directional IRF 520, capable of handling a single motor at a time. L298dn is used to operate the two side-mounted thrusters, while IRF 520 drives the top-mounted thruster.

For effective control and maneuvering, the precise orientation and position of the ROV must be recorded. This is done by using an MPU9250 sensor, which has nine degrees-of-freedom (DoFs). The degrees of freedom indicate that the sensor contains three gyroscopes, three magnetometers, and three accelerometers. The data from MPU9250 is processed on the Arduino Nano using a complimentary filter (Brzozowski et al., 2018), (Yang & Sun, 2018) to decrease noise and filter undesirable effects. The cutoff-frequency of the low-pass filter (LPF) is set by taking into account the data from the accelerometer, whilst the design of the high-pass filter is based on the signal obtained from the gyroscope measurement. Fig. 2 illustrates a schematic for the complimentary filter.

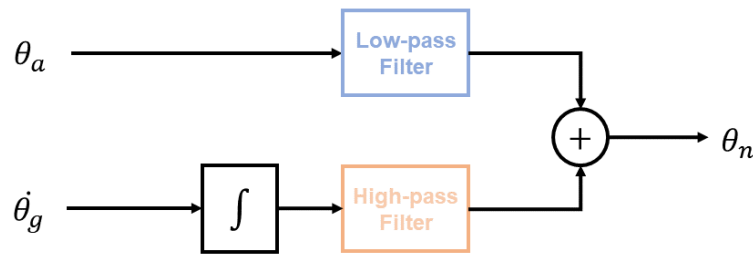


Fig. 2: An illustration of a complimentary filter in use.

By mixing data from the accelerometer and gyroscope, the expression for the complimentary filter is obtained:

$$\theta_n = (1 - \alpha)(\theta_{n-1} + \dot{\theta}_g dt) + (\alpha\theta_a) \tag{1}$$

$$\alpha = t_c / (t_c + 1/f_s) \tag{2}$$

Where,  $\theta_n$  is the current output,  $\theta_{n-1}$  is the previous output,  $\dot{\theta}_g$  is the gyroscope data,  $\theta_a$  is the accelerometer data,  $t_c$  is time constant and  $f_s$  is the sampling frequency.

### 2.1.1 Control Design

Since it is widely known that ROVs are vulnerable to parametric uncertainties and external disturbances, the control subsystem employed in the proposed ROV is a multi-parameter root-locus PI (MPRL-PI) controller (Tanveer & Ahmad, 2021), which has the capability of disturbance rejection. To enhance the performance of the PI controller and the stability of the ROV, it is suggested in this study that a complimentary filter be added to the MPU9250 sensor output.

The PI algorithm has the following expression in the time domain (Nise, 2020):

$$u(t) = K_p e(t) + K_i \int e(t) dt \tag{3}$$

where  $u(t)$  indicates the control signal,  $e(t) = y(t) - r(t)$  defines the position tracking error,  $r(t)$  is the intended trajectory,  $y(t)$  denotes the real trajectory, and  $K_p$  and  $K_i$  signify the proportional, and integral gains, respectively.

The block diagram of the PI controller is shown in Fig. 3. It is obvious that using the complimentary filter shown in Fig. 2 decreases noise levels at the MPU 9250 sensor's output.

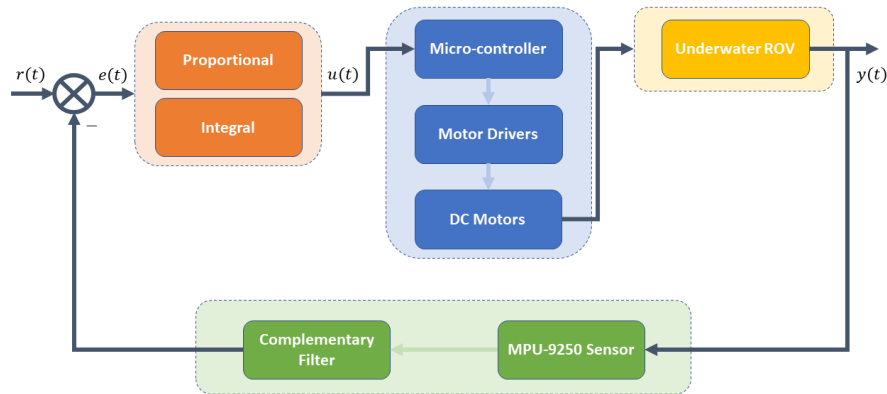


Fig. 3: PI controller block diagram with complementary filter and actuation subsystem.

The response of a MPRL-PI controller to a unit step input in heading is simulated in Fig. 4 with a sampling rate of 45 ms. It can be shown that the proposed ROV stabilizes itself when an abrupt change is induced in the input.

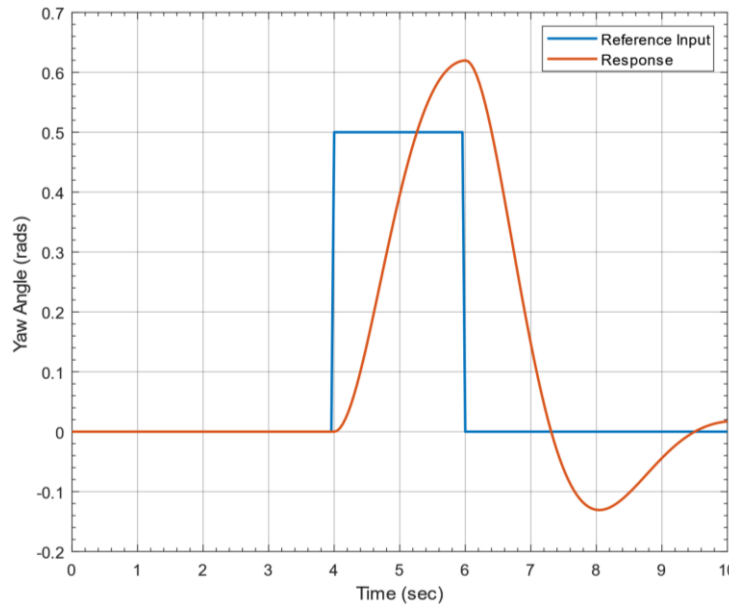


Fig. 4: Simulated response of a PID controller to a unit step input in heading.

## 2.2 Mechanical Design

The maximum depth capability of the ROV is determined by the mechanical properties of the polyvinyl chloride (PVC) utilized as a structural element in this study. Equation (4) is used to compute depth; however, it requires knowledge of the material's fracture point, equates to a pressure of 1.73 MPa. The maximum depth for a PVC pipe under these conditions is  $h = 125.65$  m.

$$P = \rho gh \tag{4}$$

where  $P$  denotes pressure,  $\rho = 1000 \text{ kg/m}^3$  signifies water density,  $g$  represents gravity, and  $h$  connotes depth in meters. Fig. 5 depicts the 3D structural architecture of the proposed ROV. The design considers buoyancy and hydrostatic factors. The structure shown incorporates a weight balancing configuration to enable implementation in the motor topology, and it was created in the SolidWorks 3D figure simulator. It measures  $35 \text{ cm} \times 26 \text{ cm} \times 23 \text{ cm}$ , weighs 1.66 kg, and an estimated volume of  $V = 1.3 \times 10^{-3} \text{ m}^3$ . This information

indicates that the buoyancy is 13.19 N, which can be calculated using Equation (5), where  $V$  is the volume, and  $E$  is the total thrust. Therefore, a maximum thrust force of 7.5 N is considered in the projected topology for the three motors.

$$E = -\rho gV \tag{5}$$

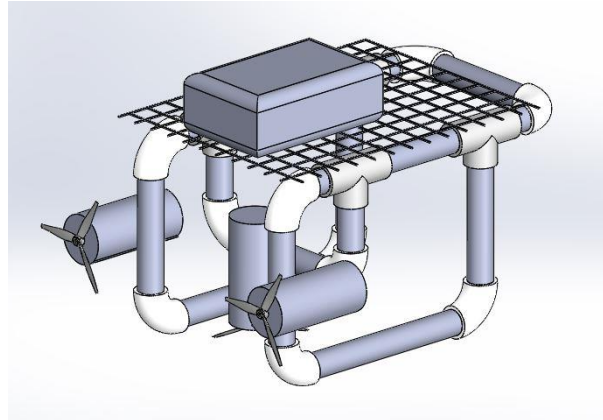


Fig. 5: 3D rendering of the envisioned ROV.

Fig. 6 depicts the placements of the three DC motors: two are situated on the front for translational and rotational motions, and one is located on top for ascending and descent movements.

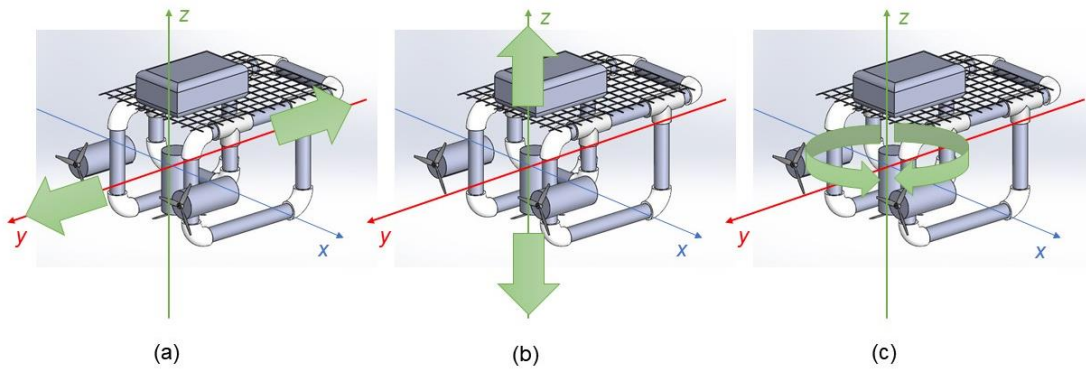


Fig. 6: ROV movements: (a) surge/translational; (b) heave/ascent-descent; (c) yaw/rotation.

The materials utilized to build the mechanical framework of the ROV are listed in Table 1. The placement of the three DC motors is made possible by the mechanical structure's design. Table 2 lists the parts and their estimated weights, which results in a total weight of 1.59 kg.

Table 1: Materials used to build the ROV structure.

Quantity (No. of Pieces)	Material Description	Size (in cm)
2	PVC Pipe	Ø1.27 x 13.9
2	PVC Pipe	Ø1.27 x 11.4
2	PVC Pipe	Ø1.27 x 10.1
1	PVC Pipe	Ø1.27 x 8.8
2	PVC Pipe	Ø1.27 x 7.6
2	PVC Pipe	Ø1.27 x 5.7
4	PVC Pipe	Ø1.27 x 4.4
6	PVC Pipe	Ø1.27 x 3.8
9	PVC Elbow	Ø1.27
9	PVC Tee	Ø1.27
1	Polypropylene Netting	30 x 18
3	Plastic Pipe Strap	Ø1.27

Table 2: The material weights for the ROV.

Item	Quantity	Weight (kg)	Total Weight (kg)
PVC structure	1	0.770	0.770
Motors	3	0.250	0.750
Motor Drivers	3	0.025	0.075
Arduino Nano	1	0.001	0.001
Sensors	2	0.001	0.002
		<b>Total Weight</b>	1.59

### 3. Experimental Results

This section provides an overview of the experimental findings utilizing the Arduino Nano as the ROV's onboard computer. The data that was recorded in a controlled aquatic setting is also presented. Additionally, the key characteristics are contrasted with those of other commercial ROVs, and the results of the implementation of the MPRL-PI controller are provided.

#### 3.1 ROV Performance

##### 3.1.1 Motor Sealing and Thruster Test Rig Design

For the ROV under consideration, a custom-built low-powered thrusters are developed using an off-the-shelf 12V DC motor. The choice of a DC motor over a BLDC motor was motivated by its low cost, ease of operation, low-cost motor drivers, and ease of sealing.

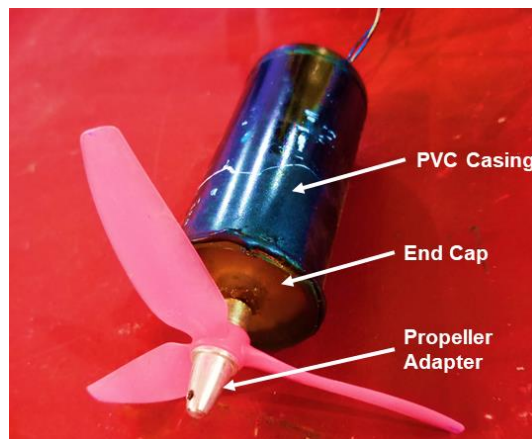


Fig. 7: The motor housed within a PVC casing.

The motors are initially wrapped in insulating tape to cover the openings at the top and sides of the motor, leaving just the shaft and connection terminals exposed. The motor housing is custom manufactured from PVC pipes, and the endcaps for the housing are fabricated from acrylic, as seen in Fig. 7. From the interior, the motor housing is covered with a thick coating of grease. Molten wax is poured into the housing once the motor is installed to fill any gaps and offer an extra layer of water protection.

A test rig is built to test the motors, and the motor step response and thrust force table are recorded. As shown in Fig. 8, a simple rectangular iron frame is built with a nut-and-bolt fastening in the centre to connect the load cell. An S-shaped 5-kg load cell is used to measure the amount of force that the motor generates underwater.

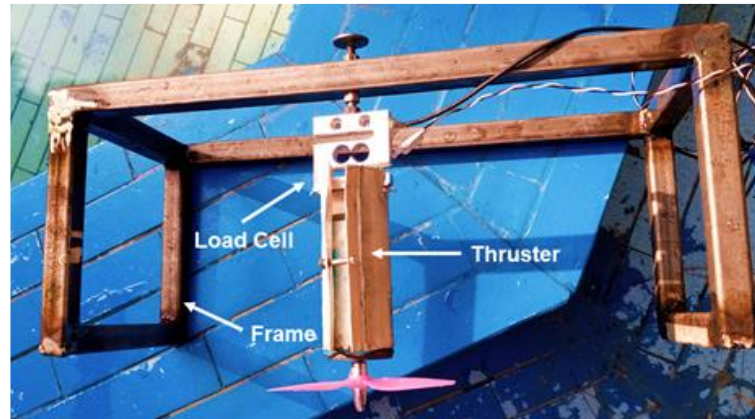


Fig. 8: Motor test rig.

### 3.1.2 Stability Performance

The ROV's orientation is tracked by the MPU9250 sensor, which is also extremely helpful in stabilizing the ROV. A smoothed signal is produced from using the complimentary filter. The data from the gyroscope is utilized in the short term since it is accurate and resistant to external influences. The accelerometer's data is used in the long-term since it did not drift. In the pool tests, the full operating ranges for gyroscope and accelerometer were  $\pm 2000$  deg/s and  $\pm 16g$ , respectively. Fig. 9 depicts motion in  $x - y$  plane. It is clear that no erratic accelerometer and gyroscope data was found, proving that they did not drift off. The complementing filter also assisted in enhancing the ROV's stability and the quality of the data that was collected.

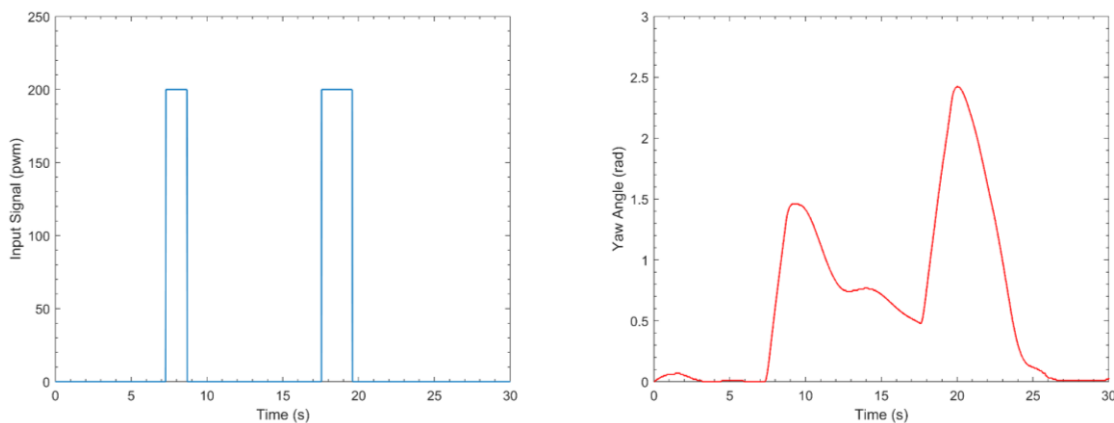


Fig. 9: Analyzing the output of the complementary filter while doing ROV stability tests.

The response of the MPRL-PI controller for yaw and heave motion can be seen in Fig. 10. It is evident that the actual trajectory followed the anticipated one. It is clear that the error was reasonably small in trajectory tracking. As a result, the ROV's stability is enhanced, which improves the quality of the gathered data.

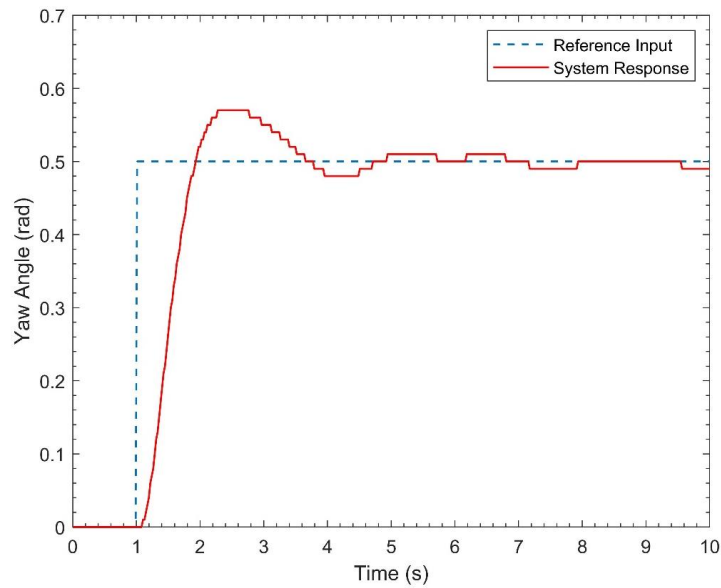


Fig. 10: MPRL-PI controller response.

### 3.1.3 Real-time Tests in Controlled Pool Environment

Fig. 11 depicts the submerged ROV in a controlled aquatic setting. In the first phase of experimentation, open-loop heave and yaw experiments were performed. ROV is given known input commands from a ground station PC. The response of the ROV against these commands is observed in real-time and stored on ground-PC. These tests also confirmed that water does not seep into the hull and that the vehicle is buoyant in water. Furthermore, the ROV has a payload capacity equal to 5% of its entire weight.

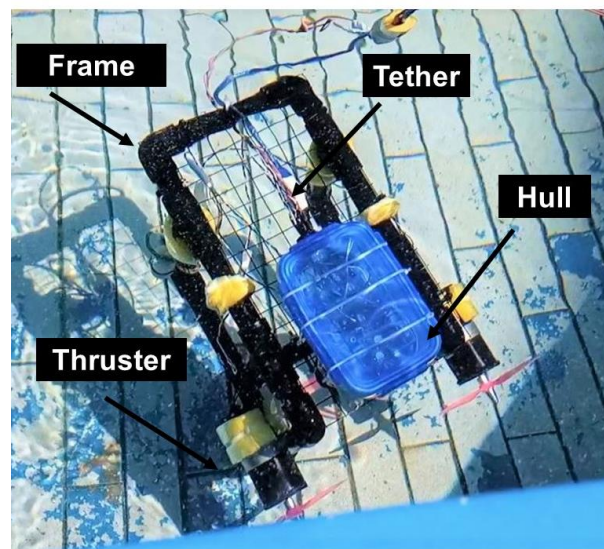


Fig. 11: A view of the submerged ROV.

### 3.1.4 In comparison to Other ROVs

Table 3 compares the capabilities of the proposed ROV to commercial ROVs. Some characteristics can be seen to be similar. However, the proposed ROV is far less expensive, allowing it to be utilized as an educational test vehicle and a low-cost inspection platform. The use of a complementary filter on IMU signals improves the performance of the MPRL-PI controller used for tracking control. The ROV's remote control is written in C++,

which is compatible with a variety of operating systems. Finally, because of the characteristics of the hardware design, the user of the proposed ROV can maintain its technological independence through the repair and replacement of mechanical and hardware components.

Table 3: Specifications of the envisaged ROV in comparison to commercial ROVs.

Features	Proposed ROV	Standard Blue ROV	UABC ROV (Aguirre-Castro et al., 2019)	Open ROV
Architecture	Open	Open	Open	Open
Maximum Depth	100	100	100	100
Endurance (in hrs)	Unlimited	2-3	2-3	2-3
Processing Type	Series	Unknown	Parallel	Unknown
Communication	Ethernet (CAT-5e)	Ethernet	Ethernet	Ethernet
Control Algorithm	MPRL-PI	PID	Smart PID	PID
Payload Capacity (% of total Weight)	05	20	20	35
Total Weight (kg)	1.59	11	15.64	2.9
Total Cost (\$)	80	2780	600	1790

#### 4. Conclusions

The article introduces the design and real-time testing of an inspection class ROV, that weighs 1.59 kg. The envisioned ROV can move in three axes of translation, ascent/descent, and rotation. The ROV was designed to reach depths of up to 100 meters, addressing the problem of human divers who can only reach depths of 30 meters. Moreover, the ROV is propelled by three DC motors controlled by a MPRL-PI controller. Improved ROV stability is achieved by using a complementary filter to reduce noise from the MPU 9250 sensor. The ROV is programmed using open-source software tools, allowing for the incorporation of additional sensors and functionality as per the operational requirements. Additionally, the adaptability of mechanical design and inexpensive hardware expands the range of possible applications, including monitoring and the research of maritime flora and fauna, without sacrificing the accuracy of the data collected.

#### Acknowledgements

The authors gratefully acknowledge the research facilities and financial support provided by Faculty of Mechanical Engineering, Ghulam Ishaq Khan Institute of Engineering Sciences and Technology, Topi 23640, Pakistan.

#### References

- Aguirre-Castro, O. A., Inzunza-González, E., García-Guerrero, E. E., Tlelo-Cuautle, E., López-Bonilla, O. R., Olguín-Tiznado, J. E., & Cárdenas-Valdez, J. R. (2019). Design and Construction of an ROV for Underwater Exploration. *Sensors*, 19(24), 5387. <https://doi.org/https://doi.org/10.3390/s19245387>
- Brito, M. P., & Griffiths, G. (2018). Updating autonomous underwater vehicle risk based on the effectiveness of failure prevention and correction. *Journal of Atmospheric and Oceanic Technology*, 35(4), 797-808. <https://doi.org/https://doi.org/10.1175/JTECH-D-16-0252.1>
- Brzozowski, B., Rochala, Z., Wojtowicz, K., & Wiczorek, P. (2018). Measurement data fusion with cascaded Kalman and complementary filter in the flight parameter indicator for hang-glider and paraglider. *Measurement*, 123, 94-101. <https://doi.org/https://doi.org/10.1016/j.measurement.2018.02.012>
- Capocci, R., Dooly, G., Omerdić, E., Coleman, J., Newe, T., & Toal, D. (2017). Inspection-class remotely operated vehicles—A review. *Journal of Marine Science and Engineering*, 5(1), 13. <https://doi.org/https://doi.org/10.3390/jmse5010013>
- Cely, J. S., Saltaren, R., Portilla, G., Yakrangi, O., & Rodriguez-Barroso, A. (2019). Experimental and computational methodology for the determination of hydrodynamic coefficients based on free decay test: Application to conception and control of underwater robots. *Sensors*, 19(17), 3631. <https://doi.org/https://doi.org/10.3390/s19173631>

- Dong, J., & Duan, X. (2023). A Robust Control via a Fuzzy System with PID for the ROV. *Sensors*, 23(2), 821. <https://doi.org/https://doi.org/10.3390/s23020821>
- Ferri, G., Munafo, A., & LePage, K. D. (2018). An autonomous underwater vehicle data-driven control strategy for target tracking. *IEEE Journal of Oceanic Engineering*, 43(2), 323-343. <https://doi.org/10.1109/JOE.2018.2797558>.
- Khojasteh, D., & Kamali, R. (2017). Design and dynamic study of a ROV with application to oil and gas industries of Persian Gulf. *Ocean Engineering*, 136, 18-30. <https://doi.org/10.1016/j.oceaneng.2017.03.014>
- Laidani, A., Boudria, M., Faci, I., Bouhamri, A., Kebdani, O., Rahmoun, L., Bellahcene, Z., & Bouhamida, M. (2022). Design and Modeling of a Low-Cost Observation Class ROV for Dam Inspection. 2022 2nd International Conference on Advanced Electrical Engineering (ICAEE),
- Li, M., Yu, C., Zhang, X., Liu, C., & Lian, L. (2023). Fuzzy adaptive trajectory tracking control of work-class ROVs considering thruster dynamics. *Ocean Engineering*, 267, 113232. <https://doi.org/10.1016/j.oceaneng.2022.113232>
- Martorell-Torres, A., Massot-Campos, M., Guerrero-Font, E., & Oliver-Codina, G. (2018). Xiroi ASV: A Modular Autonomous Surface Vehicle to Link Communications. *IFAC-PapersOnLine*, 51(29), 147-152. <https://doi.org/10.1016/j.ifacol.2018.09.484>
- Nise, N. S. (2020). *Control systems engineering*. John Wiley & Sons.
- Rafi, F., Mazhar, S., Tariq, H., Saud, M., & Rahman, M. U. (2018). Development and Testing of a Low Cost Educational Test-Bed Autonomous Underwater Vehicle for Shallow Water Observation. 2018 OCEANS-MTS/IEEE Kobe Techno-Oceans (OTO),
- Sánchez-Ferreira, C., Coelho, L., Ayala, H. V., Farias, M. C., & Llanos, C. H. (2019). Bio-inspired optimization algorithms for real underwater image restoration. *Signal Processing: Image Communication*, 77, 49-65. <https://doi.org/10.1016/j.image.2019.05.015>
- Shah, S. I. A., Khan, M., & Ahmad, S. M. (2021). Design, Development, and Fabrication of a Low Cost Remotely Operated Unmanned Underwater Vehicle. 2021 International Conference on Robotics and Automation in Industry (ICRAI),
- Shahani, K., Wu, C., Persaud, R., & Song, H. (2018). Design and control of underwater hybrid vehicle capable of performing numerous tasks. *Journal of Naval Architecture and Marine Engineering*, 15(2), 127-134. <https://doi.org/10.3329/jname.v15i2.36890>
- Tanveer, A., & Ahmad, S. (2021). Heave Modeling and Control of a Micro-ROV. 2021 International Conference on Robotics and Automation in Industry (ICRAI),
- Tanveer, A., & Ahmad, S. M. (2022). High fidelity modelling and GA optimized control of yaw dynamics of a custom built remotely operated unmanned underwater vehicle. *Ocean Engineering*, 266, 112836. <https://doi.org/10.1016/j.oceaneng.2022.112836>
- Teague, J., Allen, M. J., & Scott, T. B. (2018). The potential of low-cost ROV for use in deep-sea mineral, ore prospecting and monitoring. *Ocean Engineering*, 147, 333-339. <https://doi.org/10.1016/j.oceaneng.2017.10.046>
- Xu, R., Tang, G., Xie, D., Huang, D., & Han, L. (2018). Underactuated tracking control of underwater vehicles using control moment gyros. *International Journal of Advanced Robotic Systems*, 15(1), 1729881417750759. <https://doi.org/10.1177/1729881417750759>
- Yang, Q., & Sun, L. (2018). A fuzzy complementary Kalman filter based on visual and IMU data for UAV landing. *Optik*, 173, 279-291. <https://doi.org/10.1016/j.ijleo.2018.08.011>
- Zhang, Y.-x., Zhang, Q.-f., Zhang, A.-q., Chen, J., Li, X., & He, Z. (2022). Acoustics-Based Autonomous Docking for A Deep-Sea Resident ROV. *China Ocean Engineering*, 36(1), 100-111. <https://doi.org/10.1007/s13344-022-0009-8>